

Spontaneous emission spectrum of a two-level atom in a very high Q cavity

Alexia Auffèves¹, Benjamin Besga¹, Jean-Michel Gérard², and Jean-Philippe Poizat¹

¹*CEA/CNRS/UJF Joint team " Nanophysics and semiconductors "*,

Institut Néel-CNRS, BP 166, 25, av. des Martyrs,

38042 Grenoble Cedex 9, France and

²*CEA/CNRS/UJF Joint team " Nanophysics and semiconductors",*

*CEA/INAC/SP2M, 17 rue des Martyrs, 38054 Grenoble, France**

(Dated: November 1, 2018)

Abstract

In this paper we consider an initially excited two-level system coupled to a monomode cavity, and compute exact expressions for the spectra spontaneously emitted by each system in the general case where they have arbitrary linewidths and frequencies. Our method is based on the fact that this problem has an easily solvable classical counterpart, which provides a clear interpretation of the evidenced phenomena. We show that if the cavity linewidth is much lower than the atomic linewidth, photons are emitted at the cavity frequency, even if the atom and the cavity are strongly detuned. We also study the links between the spontaneous emission spectra and the fluorescence spectra emitted when the atom is driven by a classical field of tunable frequency in the low excitation limit.

PACS numbers: 42.50.Ct; 42.50.Gy; 42.50.Pq ; 42.65.Hw

*Electronic address: alexia.auffeves@grenoble.cnrs.fr

I. INTRODUCTION

The spontaneous emission (SE) properties of a two-level system strongly depend on its electromagnetic environment. Purcell [1] predicted first that the linewidth of an atom placed in a resonant cavity may be increased, and inhibited if the cavity is off resonance. When the atom-cavity coupling g becomes larger than the atomic and the cavity linewidths, respectively denoted γ and κ , SE becomes reversible, giving rise to the well-known vacuum Rabi oscillation [2]. These oscillations define the so-called strong coupling regime, whereas the regime where SE is irreversible is called weak coupling regime. The strong coupling regime has been reached in various systems, ranging from Rydberg atoms in microwave cavities [2], alkaline atoms in optical cavities [3, 4] to semiconducting devices [5, 6, 7, 8, 9, 10], and opens the way to the implementation of fundamental experiments in the field of quantum information. Two other regimes emerge from the comparison between the respective linewidths of the emitter γ and of the cavity κ , namely the good emitter regime (resp. the good cavity regime), fulfilling $\gamma < \kappa$ (resp. $\kappa < \gamma$). Up to now, most experiments have been conducted in the good emitter regime. Nevertheless, recent technological developments have greatly improved the quality factor Q of the cavities used in cavity quantum electrodynamics (CQED) experiments, allowing to enter the less explored regime where the cavity linewidth is of the same order of magnitude than the atomic linewidth, or even much smaller. The typical Q factor of the best optical cavities is 10^8 [3, 4], which corresponds to the linewidth of the used transition in cesium and in rubidium atoms. Q factors as high as 10^{10} have been reached in the microwave domain [11], which is ten times better than the Q factor of the transition between the considered Rydberg states. In the field of solid-state optical microcavities, Q 's above 10^8 have been achieved for silica microspheres [12] or microtoroids [13], whereas impressive progress has been recently witnessed for semiconductor based cavities such as micropillars [14], microdisks [15] or photonic crystal cavities [16]. On the emitter side, a radiative-lifetime limited emission linewidth has been observed for single semiconductor quantum dots at low temperature under resonant pumping conditions [17]. This linewidth corresponds to a typical Q of 10^6 for standard InAs self-assembled QDs ($\tau \sim 1$ ns, $\lambda \sim 1\mu\text{m}$); even smaller values in the $10^5 - 10^4$ range can be achieved for giant-oscillator-strength QDs obtained in the InGaAs/GaAs [5] or GaAs/AlAs [7, 18] systems.

After the pioneering work of Purcell, the theoretical effort to understand and model the

spectra emitted by the atom-cavity system was pursued in [19], where the emission spectrum of a Rydberg atom embedded in a cavity with no losses was computed, and the existence of the vacuum Rabi doublet was first predicted. The emission and absorption spectrum of an ideal two-level atom in a cavity with losses was studied in [20], and the fluorescence and spontaneous emission spectra emitted by a lossy atom coupled to a lossy cavity was computed in [21, 22], both systems being on resonance. Note that the problem of a two-level atom trapped in an external potential and strongly coupled to a monomode cavity is also actively studied. In particular, new and efficient cooling mechanisms have been evidenced [23, 24] and the fluorescence spectra emitted by the atom and the cavity during the cooling process have been computed [25].

In this paper, we compute exact expressions for the spectra spontaneously emitted respectively by the atom and by the cavity, in the most general case where the atom and the cavity have arbitrary linewidths and frequencies in the low excitation limit. Our results match all previous studies, providing them with a common theoretical frame, and goes beyond as it allows to investigate new unexplored regimes. Our method is based on the existence of an easily solvable classical counterpart, and offers a new insight on previously predicted phenomena like cavity induced transparency [22, 26, 27] and Rayleigh scattering [28]. To our knowledge, this is the first extensive study on the emission properties of the atom-cavity system considered as a whole and accounting for the conservation of the excitation number and energy. Moreover, the spectra emitted respectively by the atom and the cavity can be compared in the good emitter regime and in the good cavity regime defined above. The comparison is striking when the atom and the cavity are detuned. In the first case, both the atom and the cavity emit photons at the atomic frequency. On the contrary, in the second case, the spectra are dramatically different. In particular, we show that a significant fraction of photons are emitted at the cavity frequency. This apparently puzzling feature was experimentally observed by [5, 6, 7, 8, 9], the present paper suggests here a simple theoretical explanation.

The paper is organized as follows. We start in section II by computing the spontaneous emission spectrum recorded if the atom is initially excited and the cavity empty, whether one looks at the atom or at the cavity. In section III we relate these relaxation spectra to the spectra which could be obtained when one drives the atom or the cavity with a classical field. In sections IV and V we give a physical interpretation of the results, in the good

emitter regime and in the good cavity regime respectively.

II. COMPUTATION OF THE SPONTANEOUS EMISSION SPECTRA

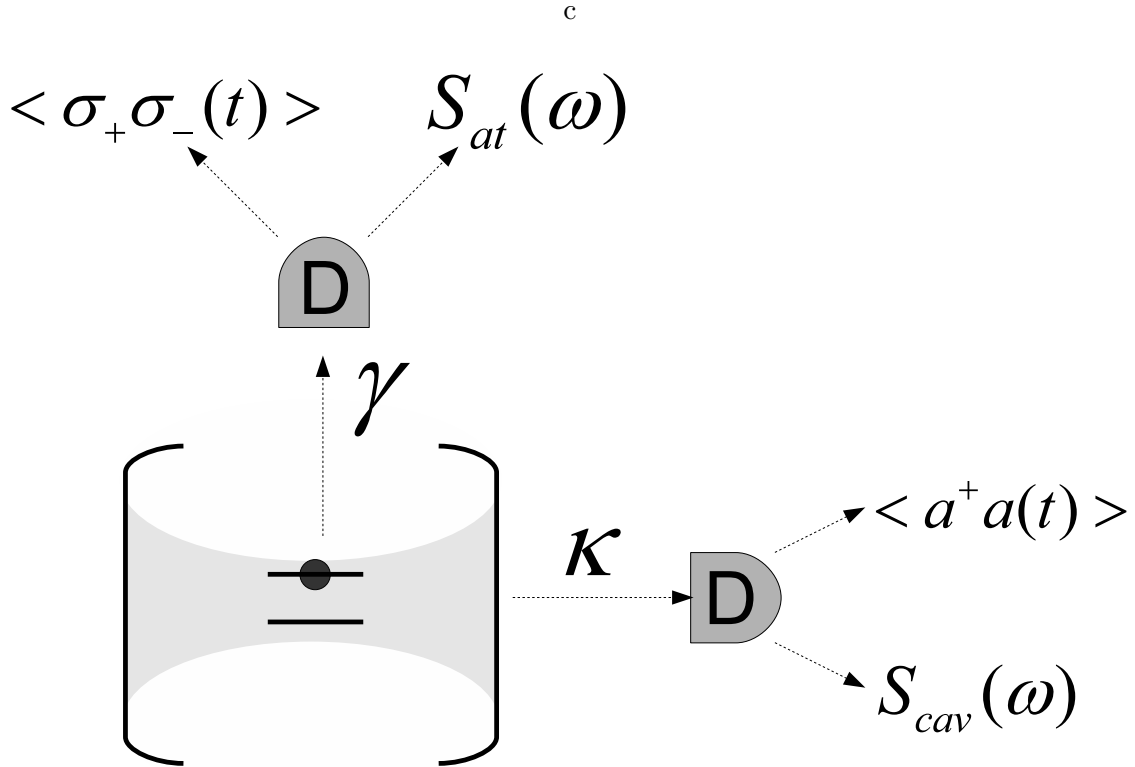


FIG. 1: *System under study. An initially excited atom is coupled to a empty cavity. Both systems have leaks characterized by the relaxation rates γ and κ . A time resolved / frequency resolved detector D is placed in the atomic (resp. cavity) channel of losses, its probability to register a photon is proportional to $\langle \sigma_+ \sigma_-(t) \rangle$ (resp. $\langle a^\dagger a(t) \rangle$) if it is time-resolved, and to $S_{at}(\omega)$ (resp. $S_{cav}(\omega)$) if it is frequency-resolved.*

In this section, we detail the method to compute the spectra spontaneously emitted by the atom, further denoted $S_{at}(\omega)$ and by the cavity, further denoted $S_{cav}(\omega)$, if the atom is initially excited and the cavity is empty, as it is depicted in figure 1. This initial state can be prepared in a wide range of experimental systems. As an example, it corresponds to the case of Rydberg atoms prepared in their excited state before they enter the mode of a 0 K microwave cavity [11]. It can also be reached if the atom and the cavity are permanently

coupled. By non-resonantly pumping a quantum dot(QD) embedded in a semiconducting cavity, one can feed the QD with a single exciton, the cavity remaining empty. Coherent excitation of a Cooper box capacitively coupled to a high Q transmission line has been realized, allowing to generate single microwave photons with high efficiency [31].

To selectively register the spectrum $S_{at}(\omega)$ or $S_{cav}(\omega)$, we connect a detector either to the atomic channel or to the cavity channel of losses. From an experimental point of view, such a distinction requires to use a cavity whose emission diagram is directional. A predominant coupling with the cavity channel of losses can be obtained by placing the detector within the emission pattern, a better coupling with the atomic channel being reached outside. As an example, the fundamental mode of a micropillar is directional, as it emits photons in a small solid angle. Consequently, it provides an efficient single photon source [32] and offers an interesting realization of solid-state one-dimensional atom [27]. Moreover, electromagnetic engineering provided by photonic crystal technology allows to control the radiation diagram of the cavities and of the leaky modes [33].

We denote ω_0 the atomic frequency, ω_{cav} the cavity frequency, $\delta = \omega_{cav} - \omega_0$ the atom-cavity detuning. The annihilation operator in the cavity mode is written a , and the atomic operators $\sigma_- = |g\rangle\langle e|$, $\sigma_+ = |e\rangle\langle g|$ and $\sigma_z = (|e\rangle\langle e| - |g\rangle\langle g|)$ where $|e\rangle$ and $|g\rangle$ are the excited and ground state of the atom respectively. We take the quantity $\omega_M = (\omega_{cav} + \omega_0)/2$ as the origin of frequencies. Energy can relax from the atom (resp. from the cavity) into a continuum of empty modes at a rate γ (resp. κ). We neglect any other dephasing processes. We can write for the operators a and σ_- the following quantum Langevin equations [29]:

$$\begin{aligned}\dot{a} &= \left(-i\frac{\delta}{2} - \frac{\kappa}{2}\right)a + g\sigma_- + F_a \\ \dot{\sigma}_- &= \left(i\frac{\delta}{2} - \frac{\gamma}{2}\right)\sigma_- + g\sigma_z a + F_s.\end{aligned}\tag{1}$$

The functions F_a and F_s are the Langevin forces allowing the conservation of the commutation relations. The spectra emitted by the atom and by the cavity fulfill [30]

$$\begin{aligned}S_{at}(\omega) &= \frac{\int dt d\tau \theta(t)\theta(t+\tau)\langle\sigma_+(t+\tau)\sigma_-(t)\rangle e^{-i\omega\tau}}{2\pi \int dt \langle S_+(t)\sigma_-(t)\rangle} \\ S_{cav}(\omega) &= \frac{\int dt d\tau \theta(t)\theta(t+\tau)\langle a^\dagger(t+\tau)a(t)\rangle e^{-i\omega\tau}}{2\pi \int dt \langle a^\dagger(t)a(t)\rangle},\end{aligned}\tag{2}$$

which can be rewritten, evidencing their reality and showing the positivity of the delay τ

$$\begin{aligned}
S_{at}(\omega) &= \frac{\int dt d\tau (\langle \sigma_+(t+\tau) \sigma_-(t) \rangle \theta(t) \theta(\tau) e^{-i\omega\tau} + cc)}{2\pi \int dt \langle S_+(t) \sigma_-(t) \rangle} \\
S_{cav}(\omega) &= \frac{\int dt d\tau (\langle a^\dagger(t+\tau) a(t) \rangle \theta(t) \theta(\tau) e^{-i\omega\tau} + cc)}{2\pi \int dt \langle a^\dagger(t) a(t) \rangle}.
\end{aligned} \tag{3}$$

In the following, we show that the correlation functions $\langle \sigma_+(t+\tau) \sigma_-(t) \rangle$ and $\langle a^\dagger(t+\tau) a(t) \rangle$ are identical to the correlation functions of two coupled cavities \mathcal{C}_1 and \mathcal{C}_2 containing classical fields whose amplitudes are respectively denoted $\alpha(t)$ and $\beta(t)$, their complex frequencies being equal to the atomic and cavity complex frequencies, $\tilde{\omega}_1 = \tilde{\omega}_{at} = -\delta/2 - i\gamma/2$, $\tilde{\omega}_2 = \tilde{\omega}_{cav} = \delta/2 - i\kappa/2$. The cavity \mathcal{C}_1 has initially been fed ($|\alpha(0)|^2 = 1$) while \mathcal{C}_2 was empty ($|\beta(0)|^2 = 0$). This problem is solved in appendix A.

We use the quantum regression theorem, which states that the evolution of the quantities $\langle \sigma_+(t+\tau) X(t) \rangle$ and $\langle a^\dagger(t+\tau) X(t) \rangle$ (where $X(t)$ describes either $a(t)$ or $\sigma_-(t)$) as a function of the delay $\tau > 0$ obeys the same equation as the expectation values $\langle \sigma_+(t) \rangle$ and $\langle a^\dagger(t) \rangle$. The initial conditions, reached for $\tau = 0$, correspond to the mean populations $\langle \sigma_+(t) X(t) \rangle$ and $\langle a^\dagger(t) X(t) \rangle$. As the average of the Langevin forces is 0, these mean values check the following equations

$$\begin{aligned}
\left\langle \frac{da}{dt} \right\rangle &= \left(-i\frac{\delta}{2} - \frac{\kappa}{2} \right) \langle a \rangle + g \langle \sigma_- \rangle \\
\left\langle \frac{d\sigma_-}{dt} \right\rangle &= \left(i\frac{\delta}{2} - \frac{\gamma}{2} \right) \langle \sigma_- \rangle + g \langle \sigma_z a \rangle
\end{aligned} \tag{4}$$

and

$$\begin{aligned}
\frac{d\langle a^\dagger a \rangle}{dt} &= -\kappa \langle a^\dagger a \rangle + g \langle \sigma_+ a \rangle + g \langle a^\dagger \sigma_- \rangle \\
\frac{d\langle \sigma_+ \sigma_- \rangle}{dt} &= -\gamma \langle \sigma_+ \sigma_- \rangle - g \langle \sigma_+ a \rangle - g \langle a^\dagger \sigma_- \rangle \\
\frac{d\langle \sigma_+ a \rangle}{dt} &= -i\delta \langle \sigma_+ a \rangle - \frac{\gamma + \kappa}{2} \langle \sigma_+ a \rangle + g \langle a^\dagger \sigma_z a \rangle + g \langle \sigma_+ \sigma_- \rangle.
\end{aligned} \tag{5}$$

The presence of the operator σ_z is responsible for the non-linear behavior of the two-level system. Nevertheless, for the initial condition we consider (namely the state $|e, 0\rangle$), the dynamics of the atom-cavity system is restricted to the subspace spanned by $|e, 0\rangle, |g, 1\rangle, |g, 0\rangle$, where we have the exact equalities $\langle \sigma_z a \rangle = -\langle a \rangle$ and $\langle a^\dagger \sigma_z a \rangle = -\langle a^\dagger a \rangle$. Note that the non-linearity induced by the operator σ_z exactly disappears. The behavior of a two-level system in a field containing at most one photon cannot be distinguished from the behavior of the two lower levels of a monomode cavity (or a harmonic oscillator) indeed. This equivalence

was exploited in [27] to compute the linear transmission of a cavity containing a two-level atom, and is the fundamental reason for the simplicity of our method.

Equations (4) are then identical to the equations describing the evolution of the classical fields' amplitudes in the two cavities \mathcal{C}_1 and \mathcal{C}_2 introduced above. In the same way, equations (5) correspond to the equations governing the energies' evolutions in \mathcal{C}_1 and \mathcal{C}_2 , with the initial conditions $|\alpha(0)|^2 = 1$ and $|\beta(0)|^2 = 0$. As announced, the quantum regression theorem allows us to conclude that the quantities $S_{at}(\omega)$ and $S_{cav}(\omega)$ correspond to the spectra $\mathcal{S}_1(\omega)$ and $\mathcal{S}_2(\omega)$ emitted by \mathcal{C}_1 and \mathcal{C}_2 during their relaxation process. Exact expressions for these spectra are computed in appendix A. We obtain after normalization

$$\begin{aligned} S_{at}(\omega) &= \frac{2((\kappa + \gamma)^2(4g^2 + \kappa\gamma) + 4\kappa\gamma\delta^2)(\kappa^2 + (\delta - 2\omega)^2)}{\pi(4g^2(\kappa + \gamma) + \kappa((\kappa + \gamma)^2 + 4\delta^2))\mathcal{D}(\omega)} \\ S_{cav}(\omega) &= \frac{2((\kappa + \gamma)^2(4g^2 + \kappa\gamma) + 4\kappa\gamma\delta^2)}{\pi(\kappa + \gamma)\mathcal{D}(\omega)}, \end{aligned} \quad (6)$$

where we have introduced the quantity

$$\mathcal{D}(\omega) = 16|\omega - \lambda_+|^2|\omega - \lambda_-|^2. \quad (7)$$

Photons are emitted by the atom-cavity system with the complex frequencies λ_+ and λ_- , where λ_+ and λ_- are the roots of the complex equation $(\omega - \tilde{\omega}_1)(\omega - \tilde{\omega}_2) - g^2 = 0$, and are studied in appendix B. If $\delta \rightarrow +\infty$, we have $\lambda_+ \rightarrow \delta/2 - i\kappa/2$, which corresponds to cavity-type photons, whereas $\lambda_- \rightarrow -\delta/2 - i\gamma/2$, which corresponds to atomic type photons. The relative weight of each peak is given by a more detailed study of the quantities $S_{cav}(\omega)$ and $S_{at}(\omega)$, which is done in the following. We stress that equations (6) generalize and match all previous results obtained on the SE of an atom in a cavity [20, 21, 22, 26].

It is interesting to relate the computed spectra to an expected experimental signal. By connecting a time-resolved detector to each channel of losses and summing both contributions, one has a density of probability $p(t)$ to register a photon, fulfilling

$$p(t) = \gamma\langle\sigma_+\sigma_-(t)\rangle + \kappa\langle a^\dagger a(t)\rangle. \quad (8)$$

We have checked that

$$\gamma \int dt \langle\sigma_+\sigma_-(t)\rangle + \kappa \int dt \langle a^\dagger a(t)\rangle = 1, \quad (9)$$

ensuring that one registers a photon with certainty. In the following, we denote $P_{at} = \gamma \int dt \langle \sigma_+ \sigma_- (t) \rangle$ and $P_{cav} = \kappa \int dt \langle a^\dagger a(t) \rangle$ the probability for the quantum of energy to escape in the atomic or in the cavity channel of losses respectively.

If the detectors are frequency-resolved, one can define the total density of probability per unit of frequency $p(\omega)$ to register a photon, fulfilling

$$p(\omega) = P_{at} S_{at}(\omega) + P_{cav} S_{cav}(\omega). \quad (10)$$

Before discussing the physical interpretation of the computed quantities, we consider in the next section the links between the spontaneous emission spectra and the fluorescence and absorption spectra registered when the atom or the cavity is driven by a classical field.

III. RELATION TO FLUORESCENCE AND ABSORPTION SPECTRA

In this section, we compare the spectra spontaneously emitted by the atom and the cavity when the atom is initially prepared in the excited state, to the spectra obtained when the atom is driven by a classical field of tunable frequency ω (atomic-type spectroscopy). The solutions in the permanent regime are searched in the frame rotating at the driving frequency, $\sigma_-(t) = \sigma_\omega e^{-i\omega t}$, $a(t) = a_\omega e^{-i\omega t}$. We pay attention to the case where the pump is too weak to saturate the two-level system, so that the fluorescence spectrum emitted by the atom is predominantly elastic. As a consequence, the spectra respectively emitted by the atom and by the cavity are proportional to $|\langle \sigma_\omega \rangle|^2$ and $|\langle a_\omega \rangle|^2$. The supplementary coupling term in the hamiltonian writes $i\hbar f(\sigma_+ e^{-i\omega t} - \sigma_- e^{i\omega t})$, which modifies the Heisenberg equation (4) for the operator σ_- in the following manner

$$\dot{\sigma}_- = \left(i\frac{\delta}{2} - \frac{\gamma}{2} \right) \sigma_- + g\sigma_z a + g\sigma_z f e^{-i\omega t} + F_s. \quad (11)$$

Remembering that the system is mostly in the state $|g, 0\rangle$, we have $\langle \sigma_z \rangle \sim -1$, while we still have $\langle \sigma_z a \rangle = -\langle a \rangle$. It is then obvious that the mean values $\langle \sigma_\omega \rangle$ and $\langle a_\omega \rangle$ follow the same evolution as the field's amplitudes α_ω and β_ω in the two cavities \mathcal{C}_1 and \mathcal{C}_2 introduced above, \mathcal{C}_1 being now driven by a classical field $f e^{-i\omega t}$. This problem is also studied in appendix A. In particular, it is shown that $|\alpha_\omega|^2$ (resp. $|\beta_\omega|^2$) is proportional to $\mathcal{S}_1(\omega)$ (resp. $\mathcal{S}_2(\omega)$). As a consequence, it is equivalent to initially excite the atom and record the spectra emitted spontaneously by the atom $S_{at}(\omega)$ and by the cavity $S_{cav}(\omega)$, or to drive the atom with a

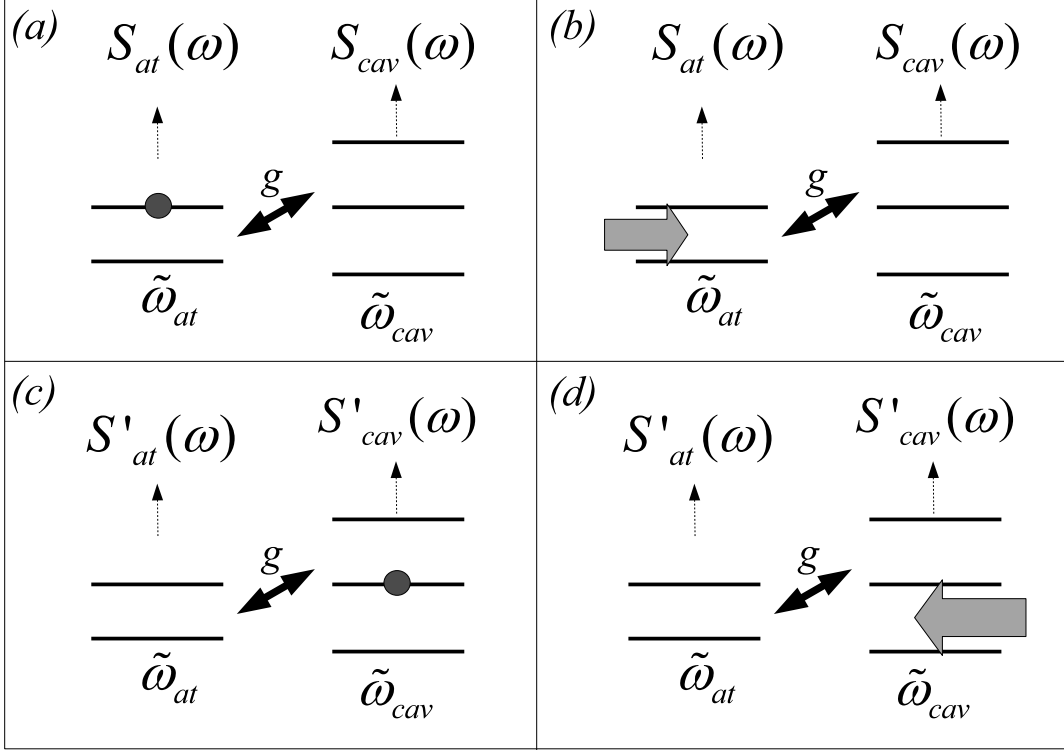


FIG. 2: A two-level atom of complex frequency $\tilde{\omega}_{at}$ is coupled to a cavity of complex frequency $\tilde{\omega}_{cav}$. (a), (b) : Atomic-type spectroscopy. The same spectra $S_{at}(\omega)$ and $S_{cav}(\omega)$ are recorded if one initially excites the atom (a) or if one drives the atom with a weak classical field (b). We have $S_{at}(\omega) = S_1(\omega)$, $S_{cav}(\omega) = S_2(\omega)$ with $\tilde{\omega}_1 = \tilde{\omega}_{at}$ and $\tilde{\omega}_2 = \tilde{\omega}_{cav}$. (c), (d) : Cavity-type spectroscopy. The same spectra $S'_{at}(\omega)$ and $S'_{cav}(\omega)$ are recorded if one initially feeds the cavity with a single photon (c) or if one drives the cavity with a weak classical field (d). Now $S'_{at}(\omega) = S_2(\omega)$, $S'_{cav}(\omega) = S_1(\omega)$ with $\tilde{\omega}_1 = \tilde{\omega}_{cav}$ and $\tilde{\omega}_2 = \tilde{\omega}_{at}$. $S_1(\omega)$ and $S_2(\omega)$ are computed in appendix A.

field of tunable frequency and to observe the elastic fluorescence field emitted by the atom and by the cavity. In the following these experiments will be referred to as "atomic-type spectroscopy". They are schematized in figures 2a and 2b.

It is interesting to check that energy is conserved when the atom is driven by a classical field. As it is shown in appendix A, energy conservation in the permanent regime has the following form

$$\gamma|\langle\sigma_\omega\rangle|^2 + \kappa|\langle a_\omega\rangle|^2 = f(\langle\sigma_\omega\rangle + \langle\sigma_\omega\rangle^*). \quad (12)$$

The two terms on the left correspond to the atomic and cavity leaks, the term on the right to the absorption of the system. These quantities are expressed in number of photons per second. Equation (12) can be rewritten in the following way, evidencing the link between the absorption spectrum and the elastic fluorescence spectra

$$f^2(P_{at}S_{at}(\omega) + P_{cav}S_{cav}(\omega)) = f(\langle\sigma_\omega\rangle + \langle\sigma_\omega\rangle^*). \quad (13)$$

It is now obvious that $f^2P_{at}S_{at}(\omega)$ (resp. $f^2P_{cav}S_{cav}(\omega)$) represents the power scattered in the atomic (resp. in the cavity) channel of losses when one drives the atom with a classical field $f e^{-i\omega t}$.

This analysis is entirely valid if the parts of the cavity and of the atom are exchanged, provided the pump's intensity is weak enough not to saturate the two-level system. This condition is mandatory indeed to make the atomic and the cavity's optical behavior indistinguishable as it is explained in section II. In this case, it is equivalent to drive the cavity mode and to register the field respectively radiated by the atom $S'_{at}(\omega)$ or by the cavity $S'_{cav}(\omega)$ (cavity-type spectroscopy), or to initially feed the cavity with a single photon and to observe the spectra spontaneously emitted by the atom or the cavity. Note that this last experiment is quite delicate as it requires the ability to prepare the cavity field in a Fock state [34]. Now we have $S'_{cav}(\omega) = S_1(\omega)$ and $S'_{at}(\omega) = S_2(\omega)$, the complex frequencies having been exchanged with respect to the previous case, $\tilde{\omega}_1 = \tilde{\omega}_{cav} + \delta/2 - i\kappa/2$, $\tilde{\omega}_2 = \tilde{\omega}_{at} = -\delta/2 - i\gamma/2$. In the following these experiments will be referred to as "cavity-type spectroscopy". They are schematized in figures 2c and 2d.

Depending on the regime we consider, four experimental situations are possible as summarized in table 14.

	Atomic-type spectroscopy	Cavity-type spectroscopy	
Good emitter	A	B	(14)
Good cavity	C	D	

Because of the symmetry between the atom and the cavity mentioned above, the situations A and D (resp. B and C) are completely equivalent. Namely, experiments A and D (resp. B and C) boil down to registering the spectrum of a cavity when it is coupled to a broader (resp. narrower) one. In section IV we discuss the spectrum emitted in an

atomic-type spectroscopy in the good emitter regime (A), before turning to the physical interpretation of the spectrum obtained in a cavity-type spectroscopy in the good cavity regime (D). In section V, we consider the spectrum obtained in an atomic-type spectroscopy operated in the good cavity regime (C), before considering the symmetrical experiment of a cavity-type spectroscopy in the good emitter regime (B).

IV. ATOMIC-TYPE SPECTROSCOPY IN THE GOOD EMITTER REGIME

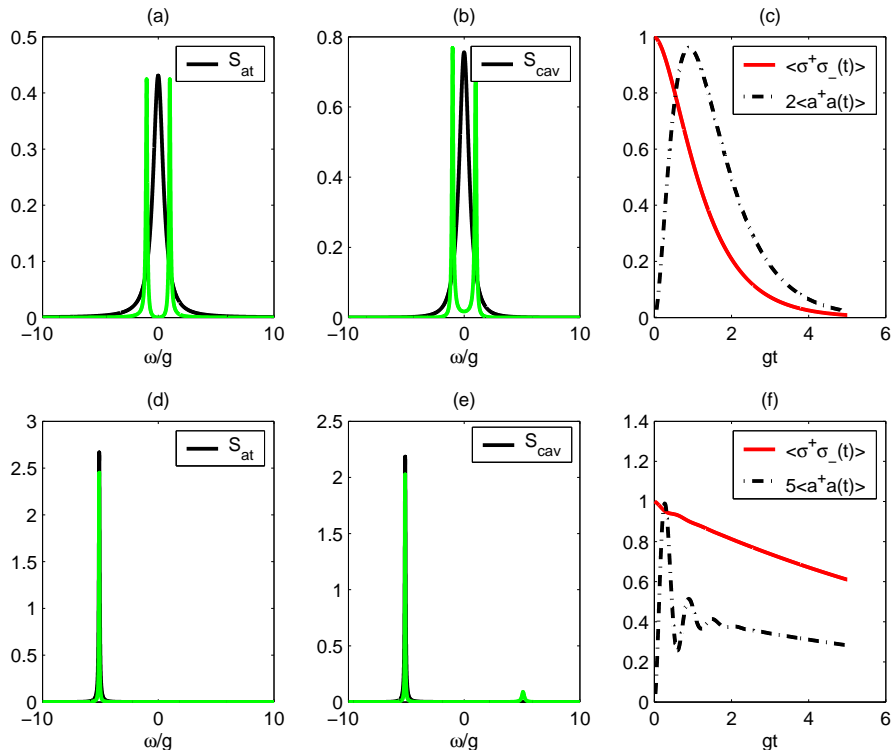


FIG. 3: Spectra emitted by the atom (a) and by the cavity (b) during an atomic-type spectroscopy in the good-emitter regime (resonant case). We took $\gamma = 0.05, g = 1$. Black line : $\kappa = 5$ (weak coupling regime). Green line : $\kappa = 0.25$ (strong coupling regime). (c) Evolution of the atomic (red solid line) and cavity (black dashed-dotted line) populations as a function of time in the weak coupling case in a SE experiment. (d), (e) and (f) : same study if the atom and the cavity are detuned. We took $\delta = 10$.

A. Resonant case

To begin with, we study the spectra $S_{at}(\omega)$ and $S_{cav}(\omega)$ emitted during an atomic-type spectroscopy in the good emitter regime, in the resonant case. As underlined above, the good emitter regime was satisfied in most experiments until now. The limit of this case consists in a perfect atom coupled to a finite bandwidth cavity, which was extensively studied in [20] and is well understood. We just recall the main results for sake of completeness.

We have represented in figures 3*a* and 3*b* the spectra S_{at} and S_{cav} in the strong coupling case (dotted line) and in the weak coupling case (solid line). We recover that in the strong coupling case, the spectra consist in the vacuum Rabi doublet evidenced in [19, 21], whereas in the weak coupling case, they reduce to a single peak. We stress that S_{at} and S_{cav} are identical. In the weak coupling case, the cavity mode can be adiabatically eliminated indeed, so that both oscillators undergo the same dynamics, leading to identical emission properties. This analysis is confirmed when one looks at figure 3*c*, where the evolution of the atomic and cavity populations is represented as a function of time. After the transient, the cavity and the atom follow the same evolution. In this picture, the cavity behaves as a relaxation channel for the atom, the coupling rate to this channel scaling like g^2/κ , as pointed out in [20]. In the case of a two-level system with very few losses ($\gamma \ll g^2/\kappa$), the coupling to the resonant cavity leads to an enhancement of the SE rate (Purcell effect [1]).

B. Non-resonant case

We have represented in figures 3*d* and 3*e* the spectra S_{at} and S_{cav} in the strong coupling case (dotted line) and in the weak coupling case (solid line) when the atom and the cavity are detuned. As it can be seen, both the atom and the cavity emit photons at the atomic frequency. The previous explanation is still valid, the cavity mode following adiabatically the atomic mode and behaving like a relaxation channel for the atom. Nevertheless, its efficiency is strongly reduced with respect to the resonant case, the coupling rate being now $g^2\kappa/\delta^2$. Note that these results can be obtained in the perturbative regime, by studying the spontaneous emission of a two-level system in a structured continuum with the Fermi-golden rule as underlined by [18].

C. Symmetrical situation

Here we analyze the physical meaning of the symmetrical experiment, namely a cavity-type spectroscopy in the good-cavity regime. As explained in section III, such an experiment can be realized by driving the cavity with a classical field of tunable frequency and registering the fluorescence spectra emitted by the atom and by the cavity, or by feeding the cavity with a single photon and recording the spontaneous emission spectra. In the frame of solid-state physics, both experiments are quite delicate, the first one requiring the ability to filtrate the pump's light, the second one the capacity to prepare the cavity in a non-classical state. The equivalent of the Purcell effect would be the enlargement of the cavity linewidth due to its coupling to the lossy atom. This enlargement is simply due to the fact that the field in the cavity mode can efficiently be scattered in the atomic channel of losses.

V. ATOMIC-TYPE SPECTROSCOPY IN THE GOOD CAVITY REGIME

A. Resonant case

We come to the interpretation of an atomic-type spectroscopy experiment held in the good-cavity regime, $\gamma > \kappa$. As it is shown in introduction, this regime is reached in an ever increasing number of experiments belonging to a wide range of systems, thanks to recent progress in the production of high Q cavities. We focus on the resonant case first. We have represented in figure 4a and 4b the spectra emitted by the atom and by the cavity in the strong coupling regime (dotted line) and in the weak coupling regime (solid line). As previously, in the strong coupling regime, both spectra consist in the vacuum Rabi doublet. On the contrary, in the weak coupling regime, the spectra respectively emitted by the atom and the cavity are dramatically different. As it can be seen in figure 4a, the presence of a very high Q resonator induces a hole in the atomic spectrum, which was already pointed out by [22, 26]. In these references, the hole is attributed to a destructive interference between the driving field and the intra-cavity field, so that the atom decouples and doesn't fluoresce anymore. This phenomenon was referred to as Cavity Induced Transparency (CIT). In a classical picture, it can be attributed to a double resonance effect, happening if one drives a broad cavity, coupled to a narrow cavity. Our computation of the atomic and cavity populations as functions of time, which is represented in figure 4c, offers a new insight on

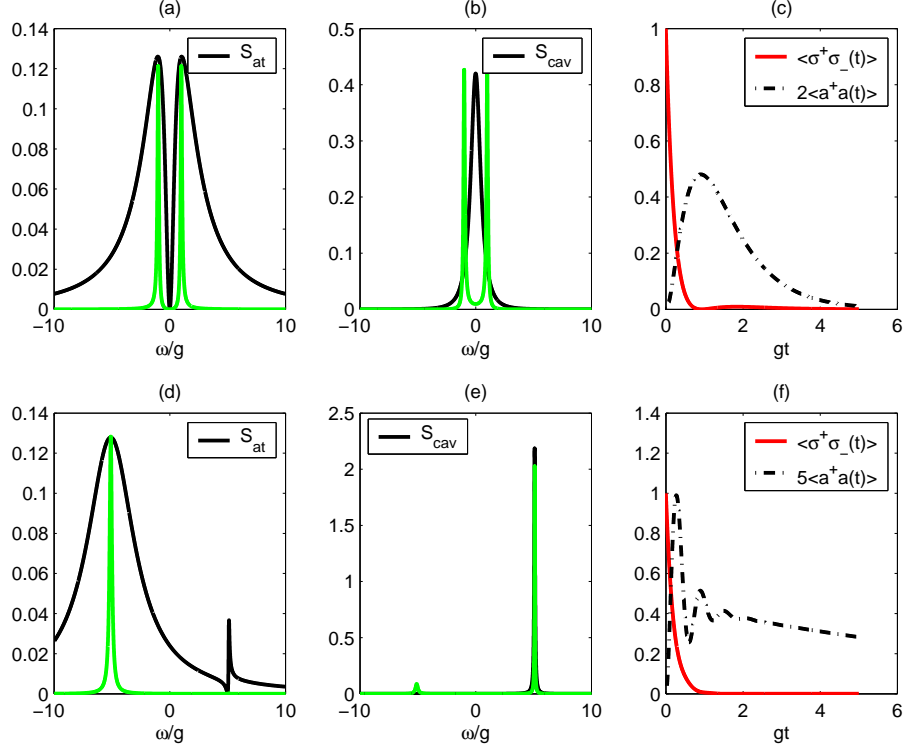


FIG. 4: Spectra emitted by the atom (a) and by the cavity (b) during an atomic-type spectroscopy in the good-cavity regime (resonant case). We took $\kappa = 0.05, g = 1$. Black line : $\gamma = 5$ (weak coupling regime). Green line : $\gamma = 0.25$ (strong coupling regime). (c) Evolution of the atomic (red solid line) and cavity (black dashed-dotted line) populations as a function of time in the weak coupling case in a SE experiment. (d), (e) and (f) : same study in the case where the atom and the cavity are detuned. We took $\delta = 10$.

CIT in the context of a spontaneous emission experiment. Contrary to what happens in the bad cavity case, the cavity evolves much slower than the atom, trapping the fraction of photon that is resonant with it, before re-emitting it in its own channel of losses. The spectrum emitted by the cavity $S_{cav}(\omega)$ is a peak of typical width $4g^2/\gamma$, which is much lower than γ . The cavity behaves thus as a very narrow spectral filter.

B. Non-resonant case

We come to the case where the atom and the cavity are detuned. As before, the analysis presented in this paragraph is valid in the strong and the weak coupling regime. One can

see in figure 4d that the atom still emits photons at its own frequency. On the contrary, as it appears in figure 4e, $S_{cav}(\omega)$ is a peak centered around the cavity frequency, which is totally different from what happens in the good emitter regime. Like in the resonant case, the cavity traps the fraction of photon resonant with it and reemit it in its own channel of losses with its own characteristics (frequency and linewidth). The absorption of the atom-cavity system at the cavity frequency is usually attributed to Rayleigh scattering, which is the non resonant scattering of photons by the atom in the cavity mode, enhanced by the presence of the mirrors [28]. In a spontaneous emission picture, this can be seen as a simple dressed-state effect. The initial state of the system is $|e, 0\rangle$ indeed, which has an overlap with the "cavity-type" dressed state scaling like g^2/δ^2 , accounting for the emission of photons at this wavelength [28]. Our results go beyond this analysis, as they allow to distinguish what is emitted by the cavity from what is emitted by the atom, and show that cavity-type photons are emitted in the cavity channel of losses, whereas atomic-type photons are emitted in the atomic one. By geometrically coupling a detector predominantly to the cavity channel of losses, one can select cavity-type rather than atomic-type photons. This feature was experimentally observed for quantum dots strongly coupled to semiconducting cavities [8, 9], where a significant fraction of photons were emitted at the cavity frequency. For a more detailed analysis of these results, it will be necessary to take into account the impact of additional sources of excitonic decoherence in experimental systems.

C. Symmetrical experiment

We come to the discussion of the reversed experiment, namely the cavity-type spectroscopy in the good emitter regime. A hole in the resonance spectrum of a cavity coupled to a narrow atom has been predicted by [22]. It was also evidenced in [27], in the particular case of a one-dimensional cavity, and referred to as Dipole Induced Reflexion. Moreover, it is shown in [27] that the medium consisting in a two-level atom coupled to a directional cavity provides a giant optical non-linear medium sensitive at the single-photon level. This feature was recently observed in the case of a photonic crystal cavity strongly coupled to a single quantum dot [10].

VI. CONCLUSION

We have shown that the SE of an atom in a cavity has a classical counterpart allowing to compute exact expressions for the spectra emitted by the atom and the cavity, in the most general case where the systems have arbitrary linewidths and frequencies. The basic reason for the existence of this classical equivalent is the vanishing of the atomic non-linearity in the relevant subspace $|e, 0\rangle$, $|g, 1\rangle$, $|g, 0\rangle$. This is due to the fact that when it is weakly excited, the two states of a two-level system cannot be distinguished from the two lower states of a monomode cavity. We have evidenced the equivalence between the spontaneous emission and elastic fluorescence spectra. Our study provides all previous results with a common theoretical frame, and goes beyond as it allows to draw a comparison between the atomic and cavity spectra. The comparison is particularly striking for a detuned atom-cavity system. The spectra are identical in the good emitter regime, and dramatically different in the good cavity regime. In the first case, the cavity behaves as a relaxation channel. On the contrary, in the second case, the cavity mode can be considered as a narrow filter, trapping and reemitting a fraction of photons with its own characteristics (frequency and linewidth) in its own channel of losses. If the radiation patterns of the atomic leaky modes and of the cavity are distinguishable, it is possible to selectively detect photons at the cavity frequency. Besides its conceptual interest, this good-cavity regime could be exploited in original devices, such as spectrally-tunable single photon sources based on cavity tuning.

VII. ACKNOWLEDGMENT

This work was supported by the Agence Nationale de la Recherche under the project IQ-Nona.

APPENDIX A: CLASSICAL COUPLED CAVITIES

In this appendix we compare the relaxation and the fluorescence spectra emitted by two coupled cavities \mathcal{C}_1 and \mathcal{C}_2 . We denote α and β the complex amplitudes of the field in each cavity, $\tilde{\omega}_1$ and $\tilde{\omega}_2$ their respective complex frequencies, and g the coupling strength between the two cavities. We define the Fourier transform $\tilde{\psi}(\omega)$ of a function $\psi(t)$ in the following way

$$\tilde{\psi}(\omega) = \frac{1}{2\pi} \int dt \psi(t) e^{i\omega t} \quad (\text{A1})$$

First we consider the relaxation of the total system when the first cavity is fed with a classical field at time $t = 0$. The evolution of the system is described by the set of equations

$$\begin{aligned} \dot{\alpha} + i\tilde{\omega}_1\alpha + g\beta &= 0 \\ \dot{\beta} + i\tilde{\omega}_2\beta - g\alpha &= 0, \end{aligned} \quad (\text{A2})$$

the initial conditions being $\alpha(0) = 1$ and $\beta(0) = 0$. The solutions are linear combinations of exponential functions at the eigenfrequencies λ_+ and λ_- , where λ_+ and λ_- are the roots of the equation $(\lambda - \tilde{\omega}_1)(\lambda - \tilde{\omega}_2) - g^2 = 0$. Their form is studied in appendix B.

Taking into account the initial conditions we find

$$\begin{aligned} \alpha(t) &= \frac{\lambda_+ - \tilde{\omega}_2}{\lambda_+ - \lambda_-} e^{-i\lambda_+ t} - \frac{\lambda_- - \tilde{\omega}_2}{\lambda_+ - \lambda_-} e^{-i\lambda_- t} \\ \beta(t) &= \frac{ig}{\lambda_+ - \lambda_-} (e^{-i\lambda_+ t} - e^{-i\lambda_- t}). \end{aligned} \quad (\text{A3})$$

One denotes $S_1(\omega)$ and $S_2(\omega)$ the spectra emitted by each cavity during the relaxation process, fulfilling (Wiener-Khinchine theorem)

$$\begin{aligned} S_1(\omega) &= \frac{|\tilde{\alpha}(\omega)|^2}{\int d\omega |\tilde{\alpha}(\omega)|^2} = \frac{\int dt d\tau \alpha^*(t + \tau) \alpha(t)}{2\pi \int dt |\alpha(t)|^2} \\ S_2(\omega) &= \frac{|\tilde{\beta}(\omega)|^2}{\int d\omega |\tilde{\beta}(\omega)|^2} = \frac{\int dt d\tau \beta^*(t + \tau) \beta(t)}{2\pi \int dt |\beta(t)|^2} \end{aligned} \quad (\text{A4})$$

From equations (A3), one easily finds

$$\begin{aligned} \tilde{\alpha}(\omega) &= \frac{-i}{\lambda_+ - \lambda_-} \left[\frac{\lambda_+ - \tilde{\omega}_2}{\lambda_+ - \omega} - \frac{\lambda_- - \tilde{\omega}_2}{\lambda_- - \omega} \right] \\ \tilde{\beta}(\omega) &= \frac{g}{\lambda_+ - \lambda_-} \left[\frac{1}{\lambda_+ - \omega} - \frac{1}{\lambda_- - \omega} \right]. \end{aligned} \quad (\text{A5})$$

which allows us to get, up to a normalization factor,

$$\begin{aligned} S_1(\omega) &\equiv \frac{1}{|\lambda_+ - \lambda_-|^2} \left| \frac{\lambda_+ - \tilde{\omega}_2}{\lambda_+ - \omega} - \frac{\lambda_- - \tilde{\omega}_2}{\lambda_- - \omega} \right|^2 \\ S_2(\omega) &\equiv \frac{1}{|\lambda_+ - \lambda_-|^2} \left| \frac{1}{\lambda_+ - \omega} - \frac{1}{\lambda_- - \omega} \right|^2. \end{aligned} \quad (\text{A6})$$

We focus now on the case where the first cavity is driven at the frequency ω . The set of equations describing the dynamics of the system writes now

$$\begin{aligned}
\dot{\alpha} + i\tilde{\omega}_1\alpha + g\beta &= fe^{-i\omega t} \\
\dot{\beta} + i\tilde{\omega}_2\beta - g\alpha &= 0.
\end{aligned}
\tag{A7}$$

f is taken real. The solutions in the permanent regime have the form $\alpha(t) = \alpha_\omega e^{-i\omega t}$ and $\beta(t) = \beta_\omega e^{-i\omega t}$. Recalling the equality $(\omega - \tilde{\omega}_1)(\omega - \tilde{\omega}_2) - g^2 = (\omega - \lambda_+)(\omega - \lambda_-)$, we immediately have

$$\begin{aligned}
\alpha_\omega &= \frac{i(\omega - \tilde{\omega}_2)f}{(\omega - \lambda_+)(\omega - \lambda_-)} \\
\beta_\omega &= \frac{-gf}{(\omega - \lambda_+)(\omega - \lambda_-)}.
\end{aligned}
\tag{A8}$$

Note that equations (A5) can be rewritten

$$\begin{aligned}
\tilde{\alpha}(\omega) &= \frac{i(\tilde{\omega}_2 - \omega)}{(\lambda_+ - \omega)(\lambda_- - \omega)} \\
\tilde{\beta}(\omega) &= \frac{-g}{(\lambda_+ - \omega)(\lambda_- - \omega)},
\end{aligned}
\tag{A9}$$

showing that $\tilde{\alpha}(\omega) \propto \alpha_\omega$ and $\tilde{\beta}(\omega) \propto \beta_\omega$. The spectra emitted by each cavity being respectively proportional to $|\alpha_\omega|^2$ and $|\beta_\omega|^2$, they also correspond to $\mathcal{S}_1(\omega)$ and $\mathcal{S}_2(\omega)$. As a consequence, it is equivalent to initially feed the first cavity with a classical field and to observe the spectra emitted by each cavity $\mathcal{S}_1(\omega)$ and $\mathcal{S}_2(\omega)$ during the relaxation process, or to drive the first cavity with a classical field and to observe the fluorescence spectra radiated by each cavity. The corresponding experiments are schematized in figure 5.

Finally it is interesting to check energy conservation of the system. In the permanent regime its energy is constant and equals $E_\omega = |\alpha_\omega|^2 + |\beta_\omega|^2$, where we have expressed E_ω in number of photons. We have

$$\frac{dE_\omega}{dt} = 0 = i(\tilde{\omega}_1^* - \tilde{\omega}_1)|\alpha_\omega|^2 + i(\tilde{\omega}_2^* - \tilde{\omega}_2)|\beta_\omega|^2 + f(\alpha_\omega + \alpha_\omega^*).
\tag{A10}$$

The first two terms represent the leaks of each cavity. The third term exactly balances the leaks and corresponds to the absorption of the system.

APPENDIX B: EIGENFREQUENCIES

In this appendix we study the eigenfrequencies λ_+, λ_- of the coupled cavities system. They fulfil

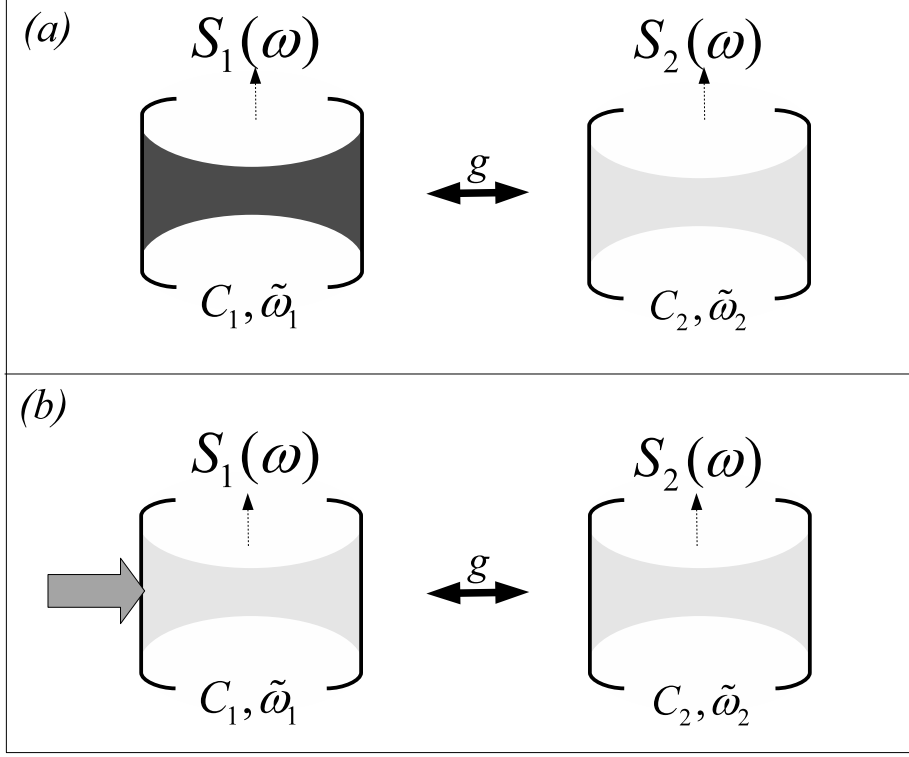


FIG. 5: Two cavities C_1 and C_2 of respective complex frequencies $\tilde{\omega}_1$ and $\tilde{\omega}_2$ are coupled with a strength g . C_1 (resp. C_2) emits the spectrum $S_1(\omega)$ (resp. $S_2(\omega)$), whether C_1 is initially fed with a classical field (a), or if it is driven with a classical field of tunable frequency (b).

$$\begin{aligned}\lambda_+ + \lambda_- &= \tilde{\omega}_1 + \tilde{\omega}_2 \\ \lambda_+ \lambda_- &= \tilde{\omega}_1 \tilde{\omega}_2 - g^2\end{aligned}\tag{B1}$$

In the resonant case, we have $\lambda_{\pm} = i\frac{\kappa+\gamma}{4} \pm \sqrt{g^2 - \left(\frac{\kappa-\gamma}{4}\right)^2}$. The system has two distinct oscillation frequencies if $4g > |\kappa - \gamma|$, as pointed out by Andreani and coworkers [18]. This is the case in the strong coupling regime defined as $g \gg \kappa, \gamma$, where the eigenfrequencies of the system are simply $\pm g$. In the general case the solutions can be written $\lambda_{\pm} = \pm \frac{a}{2} - i\frac{b_{\pm}}{2}$, with

$$\begin{aligned}
a^2 &= 2g^2 + \frac{\delta^2}{2} - \frac{1}{2} \left(\frac{\kappa - \gamma}{2} \right)^2 + \sqrt{\left(2g^2 - \frac{1}{2} \left(\frac{\kappa - \gamma}{2} \right)^2 \right)^2 + \delta^2 \left(2g^2 - \frac{1}{2} \left(\frac{\kappa - \gamma}{2} \right)^2 \right) + \left(\frac{\delta^2}{2} \right)^2} \\
b_+ &= \frac{\kappa + \delta}{2} + \frac{\delta}{2a} (\kappa - \gamma) \\
b_- &= \frac{\kappa + \delta}{2} - \frac{\delta}{2a} (\kappa - \gamma)
\end{aligned} \tag{B2}$$

If the detuning is strong $\delta \gg g, \kappa, \gamma$, we have $\lambda_+ \sim \delta/2 - i\kappa/2$, $\lambda_- \sim -\delta/2 - i\gamma/2$ and we recover the complex frequency of the undressed cavities. It is interesting to consider the limits of these expressions in the strong coupling case where $g \gg \kappa, \gamma$. After development the quantity a takes the following form

$$a^2 = \delta^2 + 4g^2 - \left(\frac{\kappa - \gamma}{2} \right)^2 \sin^2(2\theta) \tag{B3}$$

where we have introduced the mixing angle θ , checking $\tan(2\theta) = 2g/\delta$. We obtain after some little algebra $b_+ = \kappa \cos^2 \theta + \gamma \sin^2 \theta$ and $b_- = \kappa \sin^2 \theta + \gamma \cos^2 \theta$. In the strong coupling regime, the poles λ_+ and λ_- correspond to the complex frequencies of the first manifold's dressed states of the atom-cavity system as computed in [28].

-
- [1] E. M. Purcell, Phys. Rev. **69**, 681 (1946).
 - [2] M. Brune *et al.*, Phys. Rev. Lett. **76**, 1800 (1996).
 - [3] A. D. Boozer, A. Boca, R. Miller, T. E. Northup, H. J. Kimble, Phys. Rev. Lett. **98**, 193601 (2007).
 - [4] T. Puppe *et al.*, Phys. Rev. Lett. **99**, 013002 (2007), T. Wilk, S. C. Webster, A. Kuhn, and G. Rempe, Science **317**, 488-490 (2007), T. Wilk, S. C. Webster, H. P. Specht, G. Rempe, and A. Kuhn, Phys. Rev. Lett. **98**, 063601 (2007).
 - [5] J.P. Reithmaier *et al.*, Nature **432**, 197 (2004).
 - [6] T. Yoshie *et al.*, Nature **432**, 200 (2004).
 - [7] E. Peter *et al.*, Phys. Rev. Lett. **95**, 067401 (2005).
 - [8] K. Hennessy *et al.*, Nature **445**, 896 (2007).
 - [9] D. Press, S. Gotzinger, S. Reitzenstein, C. Hofmann, A. Löffler, M. Kamp, A. Forchel, and Y. Yamamoto, Phys. Rev. Lett. **98**, 117402 (2007).

- [10] D. Englund, A. Faraon, I. Fushman, N. Stoltz, P. Petroff and J. Vuckovic, *Nature* **450**, 06234 (2007).
- [11] S. Gleyzes *et al.*, *Nature* **446**, 297 (2007).
- [12] V. Sandoghdar, F. Treussart, J. Hare, V. Lefèvre-Seguin, J.-M. Raimond, S. Haroche, *Phys. Rev. A* **54**, R1777 (1996).
- [13] D. K. Armani, T.J. Kippenberg, S.M. Spillane, K.J. Vahala, *Nature* **421**, 925 (2003).
- [14] S Reitzenstein, C. Hofmann, A. Gorbunov, M. Strauss, S.H. Kwon, C. Schneider, A. Löffler, S. Höfling, M. Kamp and A. Forchel, *Appl. Phys. Lett.* **90**, 251109 (2007).
- [15] K. Srivanasan, M.Borselli, T.J. Johnson, P.E. Barclay, O. Painter, A. Stintz and S. Krishna, *Appl. Phys. Lett.* **85**, 3693 (2004).
- [16] E. Weidner, S. Combrie, A. de Rossi, N.V.Q Tran and S Cassette, *Appl. Phys. Lett.* **90**, 101118 (2007).
- [17] W Langbein, P. Borri, U Woggon, V. Stavarache, D. Reuter, A.D. Wieck, *Phys. Rev. B* **70**, 33301 (2004).
- [18] L.C. Andreani, G. Panzarini, J.M. Gérard, *Phys. Rev. B.* **60**, 13276 (1999).
- [19] J.J. Sanchez-Mondragon, N. B. Narozhny, J.H. Eberly, *Phys. Rev. Lett.* **51**, 550 (1983).
- [20] G.S. Agarwal and R.R. Puri, *Phys. Rev. A* **33**, 1757 (1986).
- [21] H. J. Carmichael, R. J. Brecha, M.G. Raizen, H. J. Kimble and Rice,P.R., *Phys. Rev. A* **40**, 5516 (1989).
- [22] P.R. Rice and R. J. Brecha, *Optics Communications* **126**, 230 (1996).
- [23] G. Hechenblaikner, M. Gangl, P. Horak, and H. Ritsch, *Phys. Rev. A* **58**, 3030 (1998).
- [24] S. Zippilli and G. Morigi, *Phys. Rev. Lett.* **95**, 143001 (2005)
- [25] M. Bienert, J.M. Torres, S. Zippilli and G. Morigi, *Phys. Rev. A* **76**, 013410 (2007).
- [26] P.M. Alsing, D.A. Cardimona and H. J. Carmichael, *Phys. Rev. A* **45**, 1793 (1992).
- [27] A. Auffèves-Garnier, C. Simon, J. M. Gérard and J. P. Poizat, *Phys. Rev. A* **75**, 053823 (2007).
- [28] S. Haroche, in *Fundamental Systems in quantum optics*, Les Houches Summer School LIII, edited by J. Dalibard, J. M. Raimond and J. Zinn-Justin (Elsevier, 1992), pp. 856.
- [29] M. Lax, *Phys. Rev* **145**, 110 (1966).
- [30] R.J. Glauber, in *Quantum Optics and Electronics*, edited by C. de Witt, A. Blandin and C. Cohen-Tannoudji (Gordon and Breach, New York, 1965), pp. 65-185.

- [31] A. A. Houck et al, Nature **449**, 328-331 (2007).
- [32] E. Moreau, I. Robert, J.M. Gérard, I. Abram, L. Manin, V. Thierry-Mieg, Appl. Phys. Lett. **79**, 2865 (2001).
- [33] S-H. Kim, S-K. Kim and Y-H. Lee, Phys. Rev. B **73**, 235117 (2006).
- [34] P. Bertet *et al*, Phys. Rev. Lett. **89**, 200402 (2002).